Corrosion protection of Cu by atomic layer deposition

Reference

Cremers Véronique, Rampelberg Geert, Baert Kitty, Abrahami Shoshan, Claes Nathalie, Milagres de Oliveira Thais, Terryn Herman, Bals Sara, Dendooven Jolien, Detavernier Christophe
Corrosion protection of Cu by atomic layer deposition
Journal of vacuum science and technology: A: vacuum surfaces and films - ISSN 0734-2101 - 37:6(2019), 060902
Full text (Publisher's DOI): https://doi.org/10.1116/1.5116136

Corrosion protection of Cu by Atomic Layer Deposition

Véronique Cremers,[1, 2] Geert Rampelberg,[1] Kitty Baert,[3] Shoshan Abrahami,[3] Nathalie Claes,[4] Thais Milagres de Oliveira,[4] Herman Terryn,[3] Sara Bals,[4] Jolien Dendooven,[1] and Christophe Detavernier[1]

1)*Department of Solid State Sciences, Ghent University, Krijgslaan 281/S1, B-9000 Ghent, Belgium*

2)*SIM vzw, Technologiepark 48, 9052 Zwijnaarde, Belgium*

3)*Research Group Electrochemical and Surface Engineering,*
Vrije Universiteit Brussel (VUB), Pleinlaan 2, 1050 Brussels,
Belgium

4)*Electron Microscopy for Materials Research (EMAT), University of Antwerp,*
Groenenborgerlaan 171, 2020 Antwerp, Belgium

(Dated: 15 August 2019)

Atomic Layer Deposition (ALD) is a vapor phase technique which is able to deposit uniform, conformal thin films with an excellent thickness control at the atomic scale. 18 nm thick Al_2O_3 and TiO_2 coatings were deposited conformaly and pinhole free onto micron-sized Cu powder, using trimethylaluminum (TMA) and tetrakis(dimethylamido)titanium(IV)(TDMAT) respectively as a precursor and de-ionized water as a reactant. The capability of the ALD coating to protect the Cu powder against corrosion was investigated. Therefore the stability of the coatings was studied in solutions with different pH in the range of 0-14, and in-situ raman spectroscopy was used to detect the emergence of corrosion products of Cu as an indication that the protective coating starts to fail.

Both ALD coatings provide good protection at standard pH values in the range of 5-7. In general, the TiO_2 coating shows a better barrier protection against corrosion than the Al_2O_3 coating. However for the most extreme pH conditions, pH 0 and pH 14, the TiO_2 coating starts also to degrade.

I. INTRODUCTION

Atomic Layer Deposition (ALD) is a chemical vapor growth method for the deposition of uniform thin films with thickness control at the atomic scale.[1,2,3,4,5] Due to the self-limiting nature of the gas-solid surface reactions in ALD, it is possible to grow highly conformal inorganic coatings onto large scale substrates with complex topologies.[6,7,8,9] In recent years, ALD has extensively been explored to study the surface functionalization of powders.[10] ALD coating of powders is used in a wide range of applications as e.g. for the protection of metal powder against oxidation[11,12], for the encapsulation of moisture sensitive powder[13] and catalytic activation.[14] In this research, we investigate the ability of ALD to protect Cu powder against corrosion.

Copper is a metal with a high thermal conductivity and is used for a wide range of applications in water plumbing and heat exchanger.[15,16,17] Copper is reasonably corrosion resistant, however it has a finite corrosion rate in pure water which causes defects over time. The corrosion rate depends on the temperature and the pH of the solution and the dissolved species in the water.[18,19,20,21] Barrier coatings are often used in order to protect the substrate against corrosion. A wide range of techniques have been used for the deposition of barrier coatings, e.g. chemical vapor deposition (CVD),[22,23,24] electrodeposition[25,26,27] and plasma treatment.[28] Recently, a lot of research has been done on ALD coatings protecting aluminum (alloys)[29,30], silver articles[31] and stainless steel[32] against corrosion. Abdulagatov et al.[33] studied ZnO, Al_2O_3, TiO_2 and Al_2O_3 layers with a capping of TiO_2 on a planar Cu substrate to prevent water corrosion. The combined ALD layer of Al_2O_3 and TiO_2 was able to protect the copper for 80 days in water at a temperature of 90°C. Daubert et al.[34] studied the stability against corrosion of different ALD coatings: Al_2O_3, TiO_2, ZnO, HfO_2, and ZrO_2. They found the best initial corrosion protection by the Al_2O_3 and HfO_2 coatings. However HfO_2 coatings showed the best film quality after an extended exposure.

In this work, we aim to deposit uniform, conformal and pinhole free layers of Al_2O_3 and TiO_2 on micron-sized Cu powder. We will investigate if the ALD coatings can protect the complex 3D-shaped powder surface against corrosion. The stability of the coatings was investigated in solutions with a pH value in the range of 0-14, using in-situ Raman spectroscopy.

II. EXPERIMENTAL

The ALD depositions were carried out in a home-built rotary pump-type ALD reactor for powders.[35,36] The powder is contained in a stainless steel container with a membrane at the front and the back. In this way, the gasses can flow through the membranes and the container, where it will react with the powder, while the powder is forced to stay in the container. During the deposition, the powder container is rotating (rotation speed of 35 rotations per minute) to ensure a proper agitation of the powder which enables the deposition of a conformal coating on the powder. Contrary to the often used fluidized bed reactors,[37] the ALD reactor used in this study is a pump-type reactor, which means that no purge gas is used to evacuate the ALD chamber after a precursor/reactant pulse. Instead, a turbomolecular pump is used to pump the reaction products and excess of precursor/reactant molecules away. In that way, the base pressure of the reactor was kept at $1\text{x}10^{-5}$ mbar.

During this research, dendritic Cu powder was used with an average particle size $< 45\mu$m. (Sigma Aldrich) The Al_2O_3 coating was deposited using TMA (trimethylaluminium, TMA, 97% Sigma Aldrich) as a precursor and de-ionized H_2O as a reactant. The partial pressure was regulated with a needle valve and kept at $1\text{x}10^{-3}$ mbar for TMA and $2\text{x}10^{-3}$ mbar for H_2O. One ALD cycle consisted of 20s TMA pulse time - 60s pump time - 20s H_2O pulse time - 60s pump time. The Al_2O_3 deposition consisted of 150 ALD cycles targeting a coating thickness of 18 nm. The titaniumoxide coating was deposited using TDMAT (tetrakis(dimethylamido)titanium(IV), 99,999%, Sigma Aldrich) as a precursor and de-ionized H_2O as a reactant. The bubbler of the TDMAT precursor was heated to 40°C, to increase the partial pressure to $5\text{x}10^{-4}$ mbar. One ALD cycle consisted of 20s TDMAT pulse time - 60s pump time - 20s H_2O pulse time - 60s pump time. The TiO_2 deposition consisted of 300 ALD cycles, targeting a coating thickness of 18 nm.

During the deposition, the temperature of the powder was kept at 100°C, using an external furnace. The precursor lines and the reactor walls were heated to 90°C to avoid the creation of coldspots, where the precursor/reactant possibly could condensate.

The presence of the coating was investigated using a FEI Quanta 200 F Scanning Electron Microscope (SEM) and Energy Dispersive X-ray spectroscopy (EDX) with the electron beam energy operated at 15 keV. To investigate the uniformity, conformality and the thickness of the coating, the coated Cu powder was studied with Transmission Electron Microscopy (TEM), using a FEI

Osiris microscope with an operating voltage at 200kV. The particles were first crushed in a solution with ethanol after which the solution is deposited on the Au-TEM grid, in order to prepare the sample for the measurements. With high angle annular dark field scanning transmission microscopy (HAADF-STEM), one can distinguish the core materials from the coating, because the intensity is proportional to Z^2 with Z the atomic number.

We also investigated the capacity of the coatings to act as a barrier to protect the powder against corrosion. Therefore, the stability of the coatings was studied at room temperature in several solutions with different pH values or anions with in-situ Raman spectroscopy. The Horiba Scientific LabRAM HR Evolution with excitation through a green laser (532nm) (max. 1mW - objective 50x) Raman spectrocope was used. The effect of extreme pH conditions was investigated, using solutions of 1M HNO_3 and NaOH, resulting in a pH value of 0 and 14 respectively. By lowering the concentration of the previous solutions, less extreme conditions could be studied. Solutions with 10^{-2}M of NaOH and HNO_3, resulted in pH conditions of 2 and 12 respectively. Solutions in an intermediate pH range are studied with solutions of 10^{-2} M $NaNO_3$ and 10^{-2} M $NaNO_3$ with 10^{-3} M NaOH resulting in a pH of 5 and 7. The effect of a chloride environment on the ALD coating was studied in a 0.5M NaCl solution (standard corrosive).

The suspensions were prepared in small bottles (5mg/ml). At different exposure times, a small amount of the Cu-powder was put on a cavity microscope slide in a drop of solution and Raman measurements had been performed.

III. RESULTS AND DISCUSSION

HAADF-STEM measurements were performed to determine whether the particles were coated in a uniform, conformal way. EDX elemental maps gave a fast indication about the presence of the coating. In Figure 1a the HAADF-STEM image and EDX mappings are shown for a Cu powder grain, coated with Al_2O_3. The mapped intensities for Al, O and Cu are shown. Al and O signals are clearly visible around the particle, confirming the presence of the Al_2O_3 coating.

In Figure 1b an HAADF-STEM image and EDX mapping are shown for a Cu particle, coated with TiO_2. The mapped intensities of Ti,O and Cu are shown. Ti and O can be observed, indicating the presence of the TiO_2 coating. Both EDX-mappings demonstrate the presence of an uniform coating.

By the combination of STEM imaging with different tilt angles and EDX analysis, one can observe

[H]

FIG. 3. Raman spectra of uncoated Cu powder (a), Cu powder coated with 18 nm of Al_2O_3 (b) and Cu powder coated with 18 nm of TiO_2 (c) suspended in a solution with pH 12.

that for both cases the ALD coating is uniform and conformal on the entire particle outer surface.

FIG. 1. HAADF-STEM image and EDX-mapping of Cu powder coated with 150 ALD cycles of TMA/H_2O (a) and 300 ALD cycles of TDMAT/H_2O (b).

FIG. 2. HAADF-STEM image of Cu powder coated with 150 cycles of TMA/H_2O (a) and 300 cycles of TDMAT/H_2O.

The thickness of the coating layers was determined based on HAADF-STEM images, as shown in Figure 2 for the Cu powder coated with Al_2O_3 (a) and the powder coated with TiO_2 (b). A clear difference in intensity between the Al_2O_3 respectively TiO_2 layer and the Cu particle, makes it possible to determine the thickness of the coating. The thickness of the coating was measured for different particles on different positions. The average coating thickness of the Al_2O_3 coating was 19.8 ± 0.7nm after a deposition of 150 ALD cycles, corresponding with a growth per cycle of 0.132 nm which is in agreement with the growth per cycle of 0.133 nm for the same ALD process under similar conditions, reported in literature.[38] The TiO_2 coating has an average thickness of 18.5 ± 0.6 nm after a deposition of 300 ALD cycles, corresponding to a growth per cycle of 0.062 nm. This value is in agreement with the growth per cycle of 0.065 nm reported for the TDMAT/H_2O depositions with similar process parameters.[39]

a. Raman spectroscopy The stability of both ALD coatings was tested under different pH conditions, in the range of pH 0 to pH 14. Raman spectroscopy was performed after several time steps. Depending on the pH of the solution and the presence of different anions, different copper corrosion products can be formed.[40] As an example, Figure 3 shows the Raman spectra (normalized) of the uncoated Cu powder (a), the Cu powder coated with Al_2O_3 (b) and the Cu powder coated with TiO_2 in a pH environment of 12. After two days, the uncoated Cu powder starts to corrode as indicated by the mixed copper oxide Cu_4O_3 detected by Raman spectroscopy. After 4 days, the Cu sample coated with Al_2O_3 turned black and a mixture of Cu_4O_3 and CuO

[H]

FIG. 4. Corrosion-stability of uncoated Cu powder (a), Cu powder coated with 18 nm of Al_2O_3 (b) and Cu powder coated with 18 nm of TiO_2 (c) exposed to solutions with a pH in the range of 0-14. A green square indicates that no corrosion products could be detected in the Raman spectra. A red dot indicates the occurence of a corrosion product in the Raman spectra.

TABLE I. Raman fingerprint of copper corrosion products.

Copper corrosion product	**Characteristic Wavenumbers (cm^{-1})**[41,42]
CuO	296 - 346 - 631
Cu_2O	218 - 410 - 630
Cu_4O_3	540
Cu_2OH_3Cl	515 - 3312 - 3354 - 3441

could be measured at the powder. Later, the CuO contribution became stronger. In contrast, the Cu powder coated with TiO_2 remains stable for 15 days, no corrosion products could be detected and no color changes could be observed. Table I gives an overview of the observed corrosion products with corresponding characteristic wavelength.

Figure 4 shows an overview of the corrosion resistance of the uncoated and coated powders suspended in a solution with a pH in the range of 0-14. A green square indicates that the powder is still resistant to the corresponding pH after the indicated time, as indicated by the absence of detectable corrosion products in the Raman spectra. A red circle indicates the presence of features related to corrosion products in the corresponding Raman spectrum.

In the nitric acid, HNO_3 (pH 0), the uncoated powder started to degrade after 1h. The Cu powder coated with Al_2O_3 dissolved completely after 20h. Only a blue solution of $Cu(NO_3)_2$ remains. After 20h, also the Cu powder coated with TiO_2 becomes darker and starts slowly to degrade by forming $Cu(NO_3)_2$.

In the NaOH solution (pH 14), the Cu powder coated with Al_2O_3 turned black after 20h and Cu_2O as corrosion product could be observed. In contrast, the Cu powder coated with TiO_2 remained reddish and no corrosion products could be identified. In a pH 2 solution, the Cu powder coated with Al_2O_3 started to degrade after 4 days and Cu_2O could be measured (after 2 days for uncoated

[H]

FIG. 5. Raman spectra of the Cu powders in an acid solution (pH 2) (a) and chloride solution (0.5 M NaCl) (b) from the moment the corrosion products have been detected.

Cu). The Cu powder coated with TiO_2 remained stable after 15 days. Only after 4 weeks, a weak Cu_2O-signal was measured. This is illustrated in Figure 5a.

In the pH 5 and 7 solutions, the blank Cu powder started to degrade after 4 days forming Cu_2O. The Cu powder coated with Al_2O_3 coating started to degrade after a week in the pH 5 solution, by forming Cu_2O. After 4 weeks, this powder started also to degrade in the pH 7 solution, reacting to CuO. In contrast, the Cu powder coated with TiO_2 remained stable for 4 weeks in these neutral solutions.

The last corrosion test in NaCl, showed the formation of $Cu_2(OH)_3Cl$ at the uncoated Cu powder after 3 days. After one week, this corrosion product plus Cu_2O is also found at the Al_2O_3 coated powder and just after 4 weeks a weak signal is noticed at the TiO_2 coated powder, as is illustrated in Figure 5b.

b. Pourbaix diagram The stability of a metal-aqueous interaction system is often summarized in a Pourbaix diagram.[40] It is a type of phase diagram, where the regions of immunity, passivation and corrosion are shown as a function of the pH (acidity) and E_h (standard hydrogen electronic potential). In the immunity region, no metal dissolution occurs, in contrast to the corrosion region where active metal dissolution occurs. In the passivation region, a protective metaloxide film is formed which prevents metal dissolution. The Pourbaix diagrams predict that the Al_2O_3 coating will only be stable for a pH range of 4-9,[43] while the TiO_2 coating will be stable for the entire pH range.[44] The studied ALD TiO_2 coating stayed stable in a pH of 2 and 12 in contrast to the Al_2O_3 coating as predicted by the pourbaix diagrams. For the solutions with the most extreme pH of 0 and 14, we would expect the TiO_2 coating to remain stable, however degradation occurs. We have to remark that Pourbaix diagrams are derived for crystalline metal(oxide)s, but the deposited ALD coatings are amorphous and have a lower density compared to bulk TiO_2, potentially explaining the reduced stability of the TiO_2 coating under the most extreme conditions.

IV. CONCLUSION

Micron-sized Cu powder was coated with circa 18 nm of Al_2O_3 and TiO_2 using a pump-type rotary ALD reactor. SEM/EDX showed the presence of the coatings and HAADF-STEM and EDX measurements illustrated the uniformity and conformality of both coatings. To investigate whether the coatings can protect the Cu powder against corrosion, the stability of the coated powder was tested in solutions with different pH values and in standard NaCl solution. In-situ Raman spectroscopy was used to detect corrosion products when the coating starts to fail and the powder begins to corrode.

For non-extreme pH values, both ALD coatings provide a good protection against corrosion, which suggests the pinhole free nature of the coating. In general a better barrier performance is found for the TiO_2 coated Cu powder. However, in the most extreme pH conditions of pH 0 and pH 14, the TiO_2 coating starts to degrade too, in contrast to bulk TiO_2 which remains stable as shown by Pourbaix diagrams in literature. The amorphous structure and the lower density of the TiO_2 ALD coating may cause this different behavior.

V. ACKNOWLEDGEMENT

The authors acknowledge financial support from the Strategic Initiative Materials in Flanders (SIM, SBO-FUNC project) and the Special Research Fund BOF of Ghent University (GOA 01G01513). J.D. acknowledges the Research Foundation Flanders (FWO-Vlaanderen) for a postdoctoral fellowship.

REFERENCES

[1] T. Suntola, “Atomic layer epitaxy,” Mater. Sci. Rep. **4**, 261 (1989).

[2] R. Puurunen, “Surface chemistry of atomic layer deposition: A case study for the trimethylaluminum/water process,” J. Appl. Phys. **97** (2005).

[3] R. Johnson, A. Hultqvist, and S. Bent, “A brief review of atomic layer deposition: From fundamentals to applications,” Mater. Today **17**, 236 (2014).

[4] S. George, “Atomic Layer Deposition: An Overview,” Chem. Rev. **110**, 111 (2010).

[5]V. Miikkulainen, M. Leskelä, M. Ritala, and R. Puurunen, "Crystallinity of inorganic films grown by atomic layer deposition: Overview and general trends," J. Appl. Phys. **113**, 021301 (2013).

[6]C. Detavernier, J. Dendooven, S. Pulinthanathu Sree, K. Ludwig, and J. Martens, "Tailoring nanoporous materials by atomic layer deposition," Chem. Soc. Rev. **40**, 5242 (2011).

[7]J. Elam, D. Routkevitch, P. Mardilovich, and S. George, "Conformal Coating on Ultrahigh-Aspect-Ratio Nanopores of Anodic Alumina by Atomic Layer Deposition," Chem. Mater. **15**, 3507 (2003).

[8]J. Dendooven, K. Devloo-Casier, M. Ide, K. Grandfield, M. Kurttepeli, K. Ludwig, S. Bals, P. Van Der Voort, and C. Detavernier, "Atomic layer deposition-based tuning of the pore size in mesoporous thin films studied by in situ grazing incidence small angle X-ray scattering," Nanoscale **6**, 14991 (2014).

[9]V. Cremers, R. Puurunen, and J. Dendooven, "Conformality in atomic layer deposition: Current status overview of analysis and modelling," Appl. Phys. Rev. **6**, 021302 (2019).

[10]D. Longrie, D. Deduytsche, and C. Detavernier, "Reactor concepts for atomic layer deposition on agitated particles: A review," J. Vac. Sci. Technol. A **32**, 010802 (2014).

[11]C.-L. Duan, Z. Deng, K. Cao, H.-F. Yin, B. Shan, and R. Chen, "Surface passivation of Fe_3O_4 nanoparticles with Al_2O_3 via atomic layer deposition in a rotating fluidized bed reactor," J. Vac. Sci. Technol. A **34**, 04C103 (2016).

[12]V. Cremers, A. Rampelberg, Barhoum, P. Walters, N. Claes, T. Milagres de Oliveira, G. Van Assche, S. Bals, J. Dendooven, and C. Detavernier, "Oxidation barrier of Cu and Fe powder by Atomic Layer Deposition," Surf. Coat. Tech. **349**, 1032 (2018).

[13]N. Avci, J. Musschoot, P. F. Smet, K. Korthout, A. Avci, C. Detavernier, and D. Poelman, "Microencapsulation of Moisture-Sensitive CaS:Eu[2+] Particles with Aluminum Oxide," J. Electrochem. Soc. **156**, J333 (2009).

[14]K. Leus, C. Krishnaraj, L. Verhoeven, V. Cremers, C. Detavernier, P. Dubruel, and P. Van Der Voort, "Catalytic carpets: Pt@MIL-101@electrospun PCL, a surprisingly active and robust hydrogenation catalyst," J. Catal. **360**, 81 (2008).

[15]I. Vargas, D. Fischer, M. Alsina, J. Pavissich, P. Pasten, and G. Pizarro, "Copper Corrosion and Biocorrosion Events in Premise Plumbing," Materials **10**, 1036 (2017).

[16]J.-G. K. J.-Y. Lee, S.-H.and Kim, "Investigation of pitting corrosion of a copper tube in a heating system," Eng. Fail. Anal. **17**, 1424 (2010).

[17] B. Lu, W. Meng, and F. Mei, "Experimental Investigation of Cu-Based, Double-Layered, Microchannel Heat Exchangers," J. Micromech. Microeng. **23**, 035017 (2013).

[18] B. Jeon, S. Sankaranarayanan, A. van Duin, and S. Ramanathan, "Atomistic Insights Into Aqueous Corrosion of Copper," J. Chem. Phys. **134**, 234706 (2011).

[19] S. Pehkonen, A. Palit, and X. Zhang, "Effect of Specific Water Quality Parameters on Copper Corrosion," Corrosion **58**, 156 (2002).

[20] Y. Feng, K. Siow, W.-K. Teo, K.-L. Tan, and A.-K. Hsieh, "Corrosion Mechanisms and Products of Copper in Aqueous Solutions at Various pH Values," Corrosion **53**, 389 (1997).

[21] N. Boulay and M. Edwards, " Role of Temperature, Chlorine, and Organic Matter in Copper Corrosion By-Product Release in Soft Water," Water. Res. **35**, 683 (2001).

[22] A. Sanjurjo, B. Wood, K. Lau, G. Tong, D. Choi, M. McKubre, H. Song, and N. Church, "Titanium-Based Coatings on Copper," Surf. Coat. Tech. **49**, 110 (1991).

[23] G. Kalita, M. Ayhan, S. Sharma, S. Shinde, D. Ghimire, K. Wakita, M. Umeno, and M. Tanemura, "Low temperature deposited graphene by surface wave plasma CVD as effective oxidation resistive barrier," Corros. Sci. **78**, 183 (2014).

[24] Y. Dong, Q. Liu, and Q. Zhou, "Corrosion behavior of Cu during graphene growth by CVD," Corros. Sci. **89**, 214 (2014).

[25] Y. Liu, S. Li, J. Zhang, J. Liu, Z. Han, and L. Ren, "Corrosion inhibition of biomimetic superhydrophobic electrodeposition coatings on copper substrate," Corros Sci. **94**, 190 (2015).

[26] P. Herrasti, A. del Rio, and J. Recio, "Electrodeposition of homogeneous and adherent polypyrrole on copper for corrosion protection," Electrochim. Acta **52**, 6496 (2007).

[27] G. He, S. Lu, W. Xu, S. Szunerits, R. Boukherroubb, and H. Zhang, "Controllable growth of durable superhydrophobic coatings on a copper substrate via electrodeposition," Phys. Chem. Chem. Phys. **17**, 10878 (2015).

[28] Y. Lin and H. Yasuda, "Effect of plasma polymer deposition methods on copper corrosion protection," J. Appl. Polym. Sci **60**, 543 (1995).

[29] M. Anderson, B. Aitchison, and D. Johnson, "Corrosion Resistance of Atomic Layer Deposition-Generated Amorphous Thin Films," ACS Appl. Mater. Inter. **8**, 30644 (2016).

[30] S. Potts, L. Schmalz, M. Fenker, B. Díaz, J. Światowska, V. Maurice, A. Seyeux, P. Marcus, G. Radnóczi, L. Tóth, and W. Kessels, "Ultra-Thin Aluminium Oxide Films Deposited by Plasma-Enhanced Atomic Layer Deposition for Corrosion Protection," J. Electrochem. Soc. **158**, C132 (2011).

[31] S. Park, G. Han, H. Choi, F. Prinz, and J. Shim, "Evaluation of atomic layer deposited alumina as a protective layer for domestic silver articles: Anti-corrosion test in artificial sweat," Appl. Surf. Sci. **441**, 718 (2018).

[32] C. Shan, X. Hou, and K.-L. Choy, "Corrosion resistance of TiO_2 films grown on stainless steel by atomic layer deposition," Surf. Coat. Tech. **202**, 2399 (2008).

[33] A. Abdulagatov, Y. Yan, J. Cooper, Y. Zhang, Z. Gibbs, A. Cavanagh, R. Yang, Y. Lee, and S. George, "Al_2O_3 and TiO_2 Atomic Layer Deposition on Copper for Water Corrosion Resistance," ACS Appl. Mater. Inter. **3**, 4593 (2011).

[34] J. Daubert, G. Hill, H. Gotsch, A. Gremaud, J. Ovental, P. Williams, C. Oldham, and G. Parsons, "Corrosion Protection of Copper Using Al_2O_3, TiO_2, ZnO, HfO_2, and ZrO_2 Atomic Layer Deposition," ACS Appl. Mater. Inter. **9**, 4192 (2017).

[35] D. Longrie, D. Deduytsche, J. Haemers, K. Driesen, and C. Detavernier, "A rotary reactor for thermal and plasma-enhanced atomic layer deposition on powders and small objects," Surf. Coat. Tech. **213**, 183 (2012).

[36] G. Rampelberg, D. Longrie, D. Deduytsche, and C. Detavernier, "Plasma enhanced atomic layer deposition on powders," ECS Transactions **64**, 51 (2014).

[37] H. Tiznado, D. Domínguez, F. Muñoz-Muñoz, J. Romo-Herrera, R. Machorro, O. E. Contreras, and G. Soto, "Pulsed-bed atomic layer deposition setup for powder coating," Powder Technol. **267**, 201 (2014).

[38] M. Groner, F. Fabreguette, J. Elam, and S. George, "Low-Temperature Al_2O_3 Atomic Layer Deposition," Chem. Mater. **16**, 639 (2004).

[39] Q. Xie, J. Musschoot, D. Deduytsche, R. Van Meirhaeghe, C. Detavernier, S. Van den Berghe, Y.-L. Jiang, G.-P. Ru, B.-Z. Li, and W.-P. Qu, "Growth Kinetics and Crystallization Behavior of TiO_2 Films Prepared by Plasma Enhanced Atomic Layer Deposition," J. Electrochem. Soc. **155**, H688 (2008).

[40] M. Pourbaix, *Atlas of Electrochemical Equilibria in Aqueous Solutions* (1st ed.; Pergamon Press: Oxford, U.K., 1966).

[41] L. Debbichi, M. Marco de Lucas, J. Pierson, and P. Krüger, "Vibrational Properties of CuO and Cu_4O_3 from First-Principles Calculations, and Raman and Infrared Spectroscopy," J. Phys. Chem. C **116**, 10232 (2012).

[42] V. Hayez, *Use of micro-Raman spectroscopy for the study of the atmospheric corrosion of copper alloys of cultural heritage*, Ph.D. thesis, Vrije Universiteit Brussel, Belgium (2006).

[43] K. Mutombo and M. Du Toit, *Arc Welding* (IntechOpen, Rijeka, 2011) p. 183.

[44] A. Scheurmann and P. MCIntyre, “Atomic Layer Deposited Corrosion Protection: A Path to Stable and Efficient Photoelectrochemical Cells,” J. Phys. Chem. Lett. **7**, 2867 (2016).

[45] E. Schindelholz, E. Spoerke, H.-D. Nguyen, J. Grunlan, S. Qin, and D. Bufford, “Extraordinary Corrosion Protection from Polymer–Clay Nanobrick Wall Thin Films,” ACS Appl. Mater. Inter. **10**, 21799 (2018).

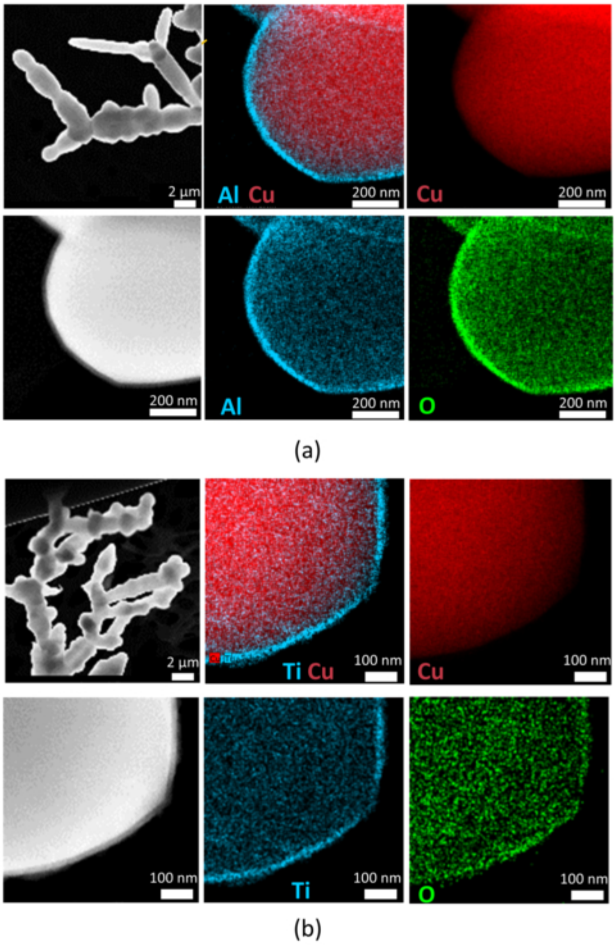
2 µm
Al Cu
200 nm
Cu
200 nm
200 nm
Al
200 nm
O
200 nm
(a)
2 µm
Ti Cu
100 nm
Cu
100 nm
100 nm
Ti
100 nm
O
100 nm
(b)

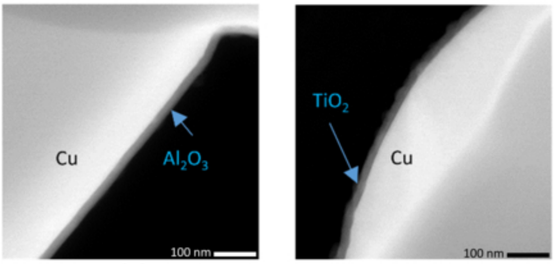

(a) (b)

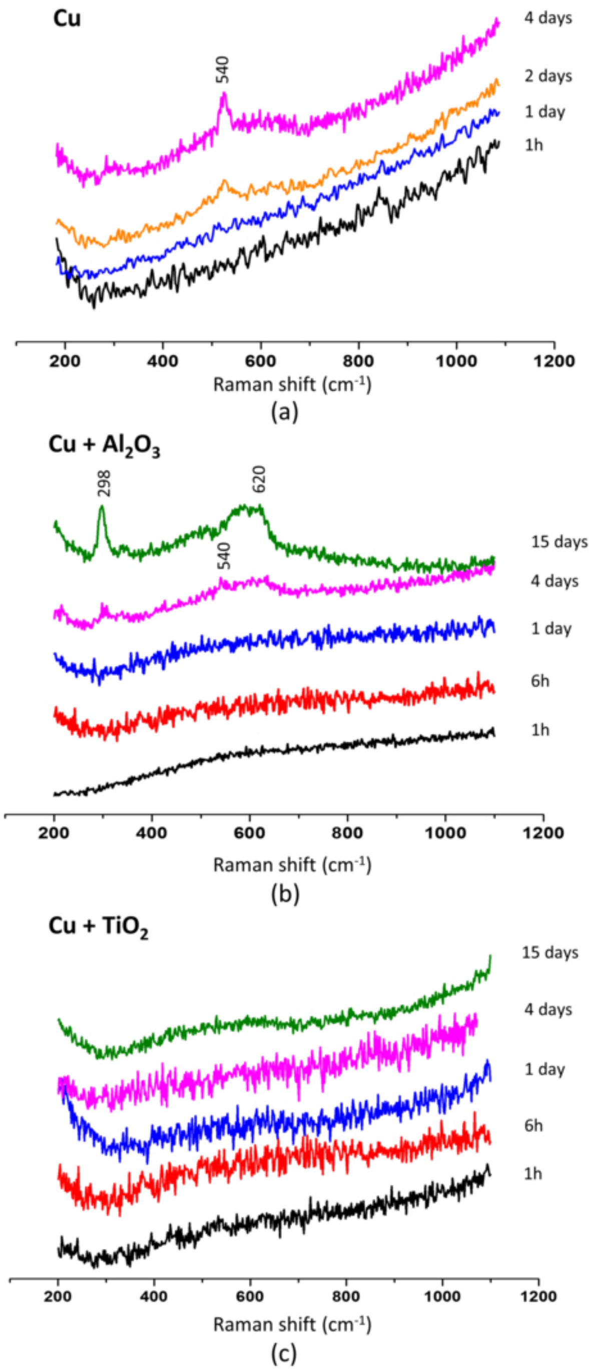
Cu
540
4 days
2 days
1 day
1h
200
400
600
800
1000
1200
Raman shift (cm-1)
(a)
Cu + Al2O3
298
620
540
15 days
4 days
1 day
6h
1h
200
400
600
800
1000
1200
Raman shift (cm-1)
(b)
Cu + TiO2
15 days
4 days
1 day
6h
1h
200
400
600
800
1000
1200
Raman shift (cm-1)
(c)

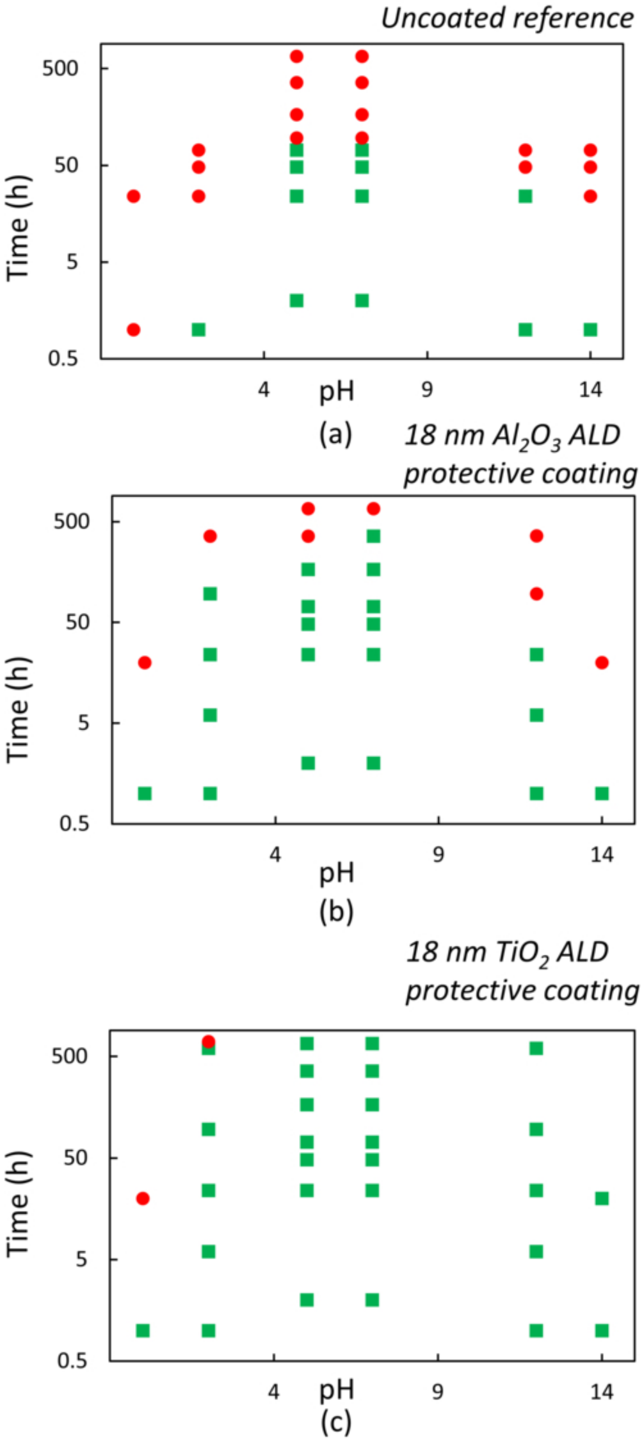
Uncoated reference
Time (h)
500
50
5
0.5
4
pH
9
14
(a)
18 nm Al_2O_3 ALD protective coating
Time (h)
500
50
5
0.5
4
pH
9
14
(b)
18 nm TiO_2 ALD protective coating
Time (h)
500
50
5
0.5
4
pH
9
14
(c)

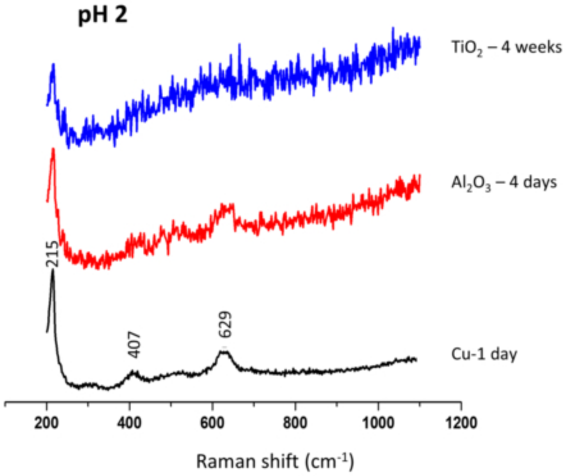
pH 2
TiO$_2$ – 4 weeks
Al$_2$O$_3$ – 4 days
Cu-1 day
215
407
629
200
400
600
800
1000
1200
Raman shift (cm^{-1})

(a)

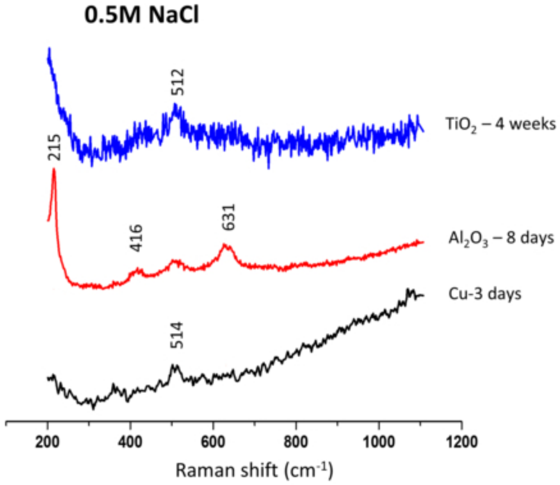
0.5M NaCl
TiO$_2$ – 4 weeks
Al$_2$O$_3$ – 8 days
Cu-3 days
512
215
416
631
514
200
400
600
800
1000
1200
Raman shift (cm^{-1})

(b)